



**STANFORD RESEARCH INSTITUTE**  
Menlo Park, California 94025 · U.S.A.

*Final Report*

*October 1977*

**DEVELOPMENT OF A VERTICAL MIXING  
DATA BASE IN THE SAN FRANCISCO BAY  
AND DELTA REGION**

**Volume I: Main Report**

*By:* P. B. RUSSELL

*Prepared for:*

STATE OF CALIFORNIA  
AIR RESOURCES BOARD  
SACRAMENTO, CALIFORNIA 95814

CONTRACT A6-066-80

SRI Project 5721

*Approved by:*

R.T.H. COLLIS, *Director*  
*Atmospheric Sciences Laboratory*

RAY L. LEADABRAND, *Executive Director*  
*Electronics and Radio Sciences Division*

*Copy No. ...11...*

LIBRARY  
AIR RESOURCES BOARD  
P. O. BOX 2815  
SACRAMENTO, CA 95812

## ABSTRACT

The objective of this project was to produce a smog-season data base on mixing depth and stability patterns in the San Francisco Bay and Delta Region, for input to air quality simulation models.

To meet this objective a network of 13 sodars (acoustic radars) was operated from mid-August to early November 1976. Ancillary measurements of temperature and humidity profiles, haze and cloud layering, and 10-m winds were made by airplane, lidar and anemometer.

Techniques of filming and manual digitization were developed to convert the continuous sodar data to hourly digital parameters describing mixing depth and near-surface echo type (a stability indicator). The sodar-inferred mixing depths were compared to those inferred from the ancillary measurements. These and previous tests show good overall agreement and demonstrate that sodar measurements compare very favorably with alternate techniques for determining mixing depth in the Bay Area. To illustrate the use of the data, time-dependent maps of mixing depth are derived for a two-day period. These maps show spatial patterns of mixing layer growth caused by solar heating of land surfaces, compensating downward motions over the bays, and the inland progression of a sudden lifting that marked the end of an air pollution incident.

Appendices include the digitized sodar, airplane, and wind data. The sodar and wind data are also available on computer cards.

This report was submitted in fulfillment of Contract A6-066-80 by SRI International under sponsorship of the California Resources Board. Work was completed as of 25 August 1977.

## DISCLAIMER

The statements and conclusions in this report are those of the Contractor and not necessarily those of the State Air Resources Board. The mention of commercial products, their source or their use in connection with material reported herein is not to be construed as either an actual or implied endorsement of such products.

## ILLUSTRATIONS

1. Contour model Showing Locations of 1976 Field Sites in the Bay and Delta Sodar Network Study . . . . .	6
2. Topography of San Francisco Bay Area . . . . .	7
3. Schematic Representation of the Monostatic Sodar Method, Equipment, and Echo Types . . . . .	8
4. Examples of Sodar Facsimile Records, Showing the Method Used to Assign Hourly Digital Echo Height and Type Parameters . . . . .	17
5. Examples of Temperature and Humidity Profiles and Inferred Mixing Depths . . . . .	22
6. Comparison of Mixing Depths Inferred from 1976 Sodar and Airplane Measurements . . . . .	23
7. Comparison Between Acoustic Echo Structure and Tower-Measured Temperature Profiles . . . . .	24
8. Comparison Between Acoustic Echo Structure and Model-Airplane-Measured Temperature Profiles . . . . .	25
9. Comparison of Mixing Depths Inferred from 1975 Sodar and Temperature-Profile Measurements . . . . .	26
10. Television Display of Simultaneously Measured Lidar and Sodar Data . . . . .	28
11. Contour Maps of Total Oxidant Measured at BAAPCD Monitoring Stations, 1330-1530 PDT, 9 and 10 October 1976 . . . . .	30
12. Contour Maps of Mixing Depth Derived From Sodar Network, 9 October 1976 . . . . .	31
13. Contour Maps of Mixing Depth Derived from Sodar Network, 10 October 1976 . . . . .	33

## TABLES

1. 1976 Sodar Network Sites . . . . .	10
2. 1976 Sodar and Wind Network Data Log . . . . .	12
3. Number and Symbol Code for Digital Sodar Data . . . . .	16
4. Sample Printout of Digital Sodar Data for One Site-Month . . . . .	19

CONTENTS

Volume I: Main Report

ABSTRACT . . . . .	i
DISCLAIMER . . . . .	i
LIST OF ILLUSTRATIONS . . . . .	iii
LIST OF TABLES . . . . .	iii
ACKNOWLEDGEMENTS . . . . .	iv
1. CONCLUSIONS . . . . .	1
2. RECOMMENDATIONS . . . . .	3
3. INTRODUCTION . . . . .	5
3.1 Background: The Problem of Determining Mixing Parameters in the San Francisco Bay Area . . . . .	5
3.2 Principles of Sodar Operation and Data Interpretation . . . . .	5
3.3 The Bay Area Sodar Network Study and its Joint Sponsorship . . . . .	9
3.4 Goals of This Study . . . . .	9
4. PROCEDURE AND METHODOLOGY . . . . .	10
4.1 Site Selection, Sodar Tests, and Network Operation . . . . .	10
4.2 Ancillary Measurements . . . . .	11
4.3 Sodar Data Processing. . . . .	11
5. DISTINCTION BETWEEN MARINE-CLASS AND LAND-CLASS DAILY SODAR RECORDS . . . . .	20
6. VALIDITY OF SODAR-INFERRED MIXING DEPTHS . . . . .	21
6.1 Relation to Temperature and Humidity Profiles . . . . .	21
6.2 Relation to Haze and Cloud Structure . . . . .	27
7. SODAR-DERIVED MIXING DEPTH MAPS FOR CONSECUTIVE HIGH AND LOW OXIDANT DAYS . . . . .	29
REFERENCES . . . . .	34
PUBLICATION RESULTING FROM THIS PROJECT . . . . .	36

Volume II: Data Appendices

APPENDIX A: Hourly Digital Mixing Depth and Stability Parameters Derived from Sodar Network Data . . . . .	1
APPENDIX B: Hourly Digital Wind Speed and Direction Data . . . . .	39
APPENDIX C: Airplane Temperature and Humidity Profiles . . . . .	57

## ACKNOWLEDGEMENTS

Many individuals and organizations contributed to the success of this research project. E. Scribner, C. Flohr, N. Nielsen, and B. Perry played major roles in selecting sites and in setting up, operating, and dismantling the 1976 sodar network. L. Gasiorek, C. Flohr, and J. Carr acquired and processed the airplane data. N. Nielsen and C. Flohr operated the lidar and photographed the lidar and sodar data. A. Smith and L. Salas digitized the sodar and wind data. H. Orthey and L. Jones produced the illustrations and text for this report.

A. Ranzieri and C. Bennett of the California Air Resources Board contributed to the experimental design, as did M. Dickerson of Lawrence Livermore Laboratory and L. Myrup of the University of California at Davis. M. Dickerson also arranged for Livermore sodar operations. J. Pryshepa of Caltrans maintained the San Francisco sodar and provided wind data. Other individuals and organizations, too numerous to mention by name, contributed to the success of the project by providing space for sodar operations on their property and by enduring the inconvenience of our activities.

We are indebted to F. Ludwig, R. Thuillier, G. Shelar, and W. Johnson for helpful discussions, and especially to E.E. Uthe for conceptualizing, initiating and supervising the Bay Area Sodar Network Study.

The first two years of the Bay Area Sodar Network Study, and a large portion of the third year (1976), were supported by Grant AEN73-02918-A01 of the National Science Foundation, Research Applications Directorate.

## 1. CONCLUSIONS

The following conclusions are based on: (1) sodar performance, and data acquired, at 13 sites in the San Francisco Bay and Delta Region during 2.5 months of the 1976 smog season, (2) extensive comparisons of the sodar data with temperature, humidity, haze, and cloud vertical profiles acquired by airplane and lidar, and (3) documented results from two previous years of the Bay Area Sodar Network Study (Russell and Uthe, 1975, 1977a,b).

- In the San Francisco Bay and Delta Region, sodar compares very favorably with alternate methods (airplane, balloon, tower, lidar) of monitoring mixing depth, especially when the shortcomings (high cost, small practical sampling rates, airspace restrictions, data ambiguities) of these alternate methods are objectively considered.
- In spite of the above, occasional measurements of temperature, humidity, haze, and cloud vertical profiles are a very useful adjunct to continuous sodar measurements, especially at new sites, seasons, or times of day.
- Techniques of filming and manual digitization of Bay Area sodar facsimile records permit compact storage, quick access, straightforward computer input, and easy human comprehension of much of the sodar-derived information on mixing depth and stability. (Digital sodar data from the 13-station network are tabulated in Appendix A and also available on computer cards for input to model calculations.)
- Time-dependent contour maps of mixing depth can readily be drawn from these digital data listings.
- These time-dependent maps confirm previous studies (e.g. Ahrens and Miller, 1969) that indicated great spatial and temporal variations in Bay Area mixing depth. The maps show, for example, patterns of mixing layer growth due to solar heating of land surfaces, compensating downward motions over the bays, and inland movement of layer growth due to marine influences.
- The data appear to show that nighttime and early morning mixing depth and stability have an important influence on both primary and secondary ground-level pollutant concentrations that occur later in the day. This tentative indication should be explored by further modeling and measurement studies. If verified, it points to one significant advantage of a continuous, unattended mixing depth and stability monitor: namely, that measurements made at nighttime, when conventional measurements are inconvenient and hence sparse, can provide important new insights to solving air quality problems.
- A Bay Area sodar network, using commercially available equipment, can produce a data capture rate of 95% or better, 24 hours per day, with no noise complaints from neighbors, provided that: (1) sites

are properly selected and enclosures properly constructed, (2) all sodar units are carefully adjusted and intercompared before deployment, (3) equipment checks at each site are made at two-day intervals; and (4) a technician and a limited supply of spare parts are kept on call for immediate servicing during normal working hours. (Equipment failures averaged about one per site per month; on-site repair time averaged about one hour per failure.)

## 2. RECOMMENDATIONS

On the basis of the foregoing conclusions we recommend that:

- The digital sodar data (on mixing depth and stability), the wind data, and the airplane data contained in Volume II (Data Appendices) should be publicized and made available to modelers for use in studies of Bay Area air quality. Both computer cards and listings should be made available. Pollution records of the Bay Area Air Pollution Control District (BAAPCD) should be scanned to select and highlight cases of greatest interest. For any days of interest on which the NSF sodar data have not been digitized, this digitization should be carried out (using the microfilmed record available) and the data should be added to the present data set. (NSF data have only been digitized for about 31 selected high-oxidant days at each site--See Appendix A.)
- The predictive value of the digital sodar data should be assessed by determining the correlation between (1) morning mixing depth and stability parameters and (2) pollutant concentrations measured later in the day. Near-surface wind data should be included in the correlation studies, and predictive equations should be derived from the time-lagged correlation coefficients.
- A mixing depth submodel, designed to derive Bay Area mixing depth fields from commonly available surface meteorological and cloud cover data, should be developed by carefully combining and analyzing the mixing depth data in this report with simultaneous surface and cloud data. This submodel could then be used to provide mixing depth inputs to Bay Area air quality models for cases where direct mixing depth measurements are incomplete or unavailable.
- The origin of nighttime spike echoes on the sodar records should be studied by making simultaneous measurements of acoustic echo structure, vertical temperature and humidity profiles, cloud cover, and infrared radiative fluxes at appropriate times. These spike echoes, which suggest nighttime convective activity, appear to be important indicators of good dilution conditions for pollutants generated at night and in the morning rush hour. They usually presage small midday and afternoon pollution concentrations. (See e.g., Russell and Uthe, 1977b.)
- A study should be conducted of the design, cost, and use of an operational Bay Area sodar network, possibly with real-time data transfer to a central point using the BAAPCD data linkup. Such an operational network could provide vital inputs to episode warning and control tactics, as well as historical data on mixing depth climatology and its alteration by increased urbanization and changing weather patterns.

- If more detailed information concerning the (bending or breaking) effect of major terrain features (ridges) on the Bay Area inversion is needed for satisfactory air quality simulations, data should be acquired with sodars located both on these ridges and in a line perpendicular to each ridge, along upwind and downwind slopes. (The coarse spacing of sodars in this study did not permit detailed study of this question.) Simultaneous tracer releases, airborne sampling, and balloon releases would provide additional data on cross-inversion transport and inversion breaks.
- Electronic techniques should be developed for automatically reducing sodar return signals in terms of the digital format developed on this project. This would greatly facilitate future research and operational sodar programs.
- Methods should be considered and developed to extend the information content derived from the sodar technique. For example, information on winds can be obtained by using Doppler or angle-of-arrival techniques, and vertical humidity information can be obtained by using differential absorption techniques.

### 3. INTRODUCTION

#### 3.1. Background: The Problem of Determining Mixing Parameters in the San Francisco Bay Area

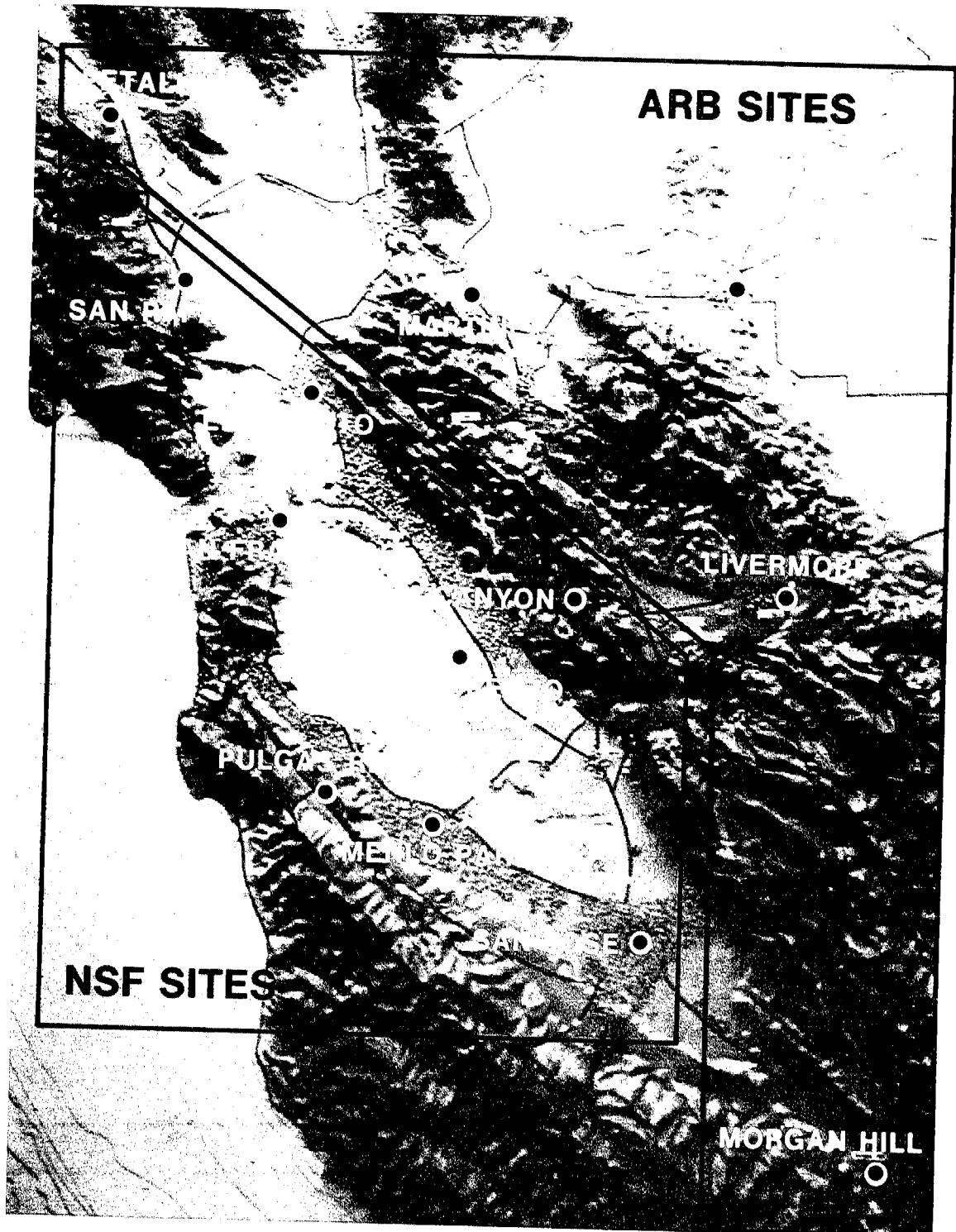
The San Francisco Bay Area is a metropolitan region of complex topography, shown in Figures 1 and 2. The region has a high incidence of strong, low inversions of two principal types: those caused by large-scale subsidence above a layer of cool marine air, and those caused by nocturnal radiative surface cooling. These inversions, interacting with the complex topography, produce fields of mixing depth and stability that can be highly variable in space and time (see, e.g., Ahrens and Miller, 1969). Hence, adequate characterization of these fields for input to air quality simulation models requires frequent measurements from a wide variety of locations. This need for complete and accurate input data sets has recently been emphasized by the development of an air quality model (the LIRAQ model--MacCracken and Sauter, 1975) that is tailored to the region and intended for use by state and local agencies in predicting the air quality consequences of proposed land uses.

Unfortunately, frequent multisite measurements using towers, airplanes, or balloons are impracticable in the Bay Area because of their great expense and air traffic restrictions. On the other hand, remote, ground-based measurements with a network of sodars (acoustic radars) offer the possibility of providing the required mixing depth and stability information economically, continuously in time, and with no obstacles to the airspace. Moreover, as the following subsections point out, this possibility is especially strong in the San Francisco Bay Area because of its special meteorology. Demonstration of this promise would permit a significant advance in developing input data sets for Bay Area air quality models.

#### 3.2. Principles of Sodar Operation and Data Interpretation

A sodar (for sound detection and ranging) operates on a backscatter principle very similar to that of radar (for radio detection and ranging). As shown in Figure 3, a pulse of sound is transmitted into the atmosphere, and the amount of sound scattered back to the sodar's antenna is measured as a function of height. Received signals are displayed on a height/time diagram, with darker areas marking the times and heights of strong acoustic backscattering.

Acoustic backscattering is caused by small-scale (about 10-cm) temperature inhomogeneities, which are produced by turbulence in regions of larger-scale potential temperature gradients. Typical combinations of turbulence and temperature gradients produce acoustic echo shapes of two major types, sometimes called layer echoes and spike echoes. As illustrated in Figure 3, layer echoes tend to be horizontal and continuous in time, while spike echoes appear as vertical, intermittent spikes or "grass" rising from the ground. Layer echoes mark regions of static stability (potential temperature,  $\theta$ , increasing with height), whereas spike echoes mark individual rising convective cells ("thermals").



SA-3442-44R2

FIGURE 1 CONTOUR MODEL SHOWING LOCATIONS OF 1976 FIELD SITES IN THE BAY AND DELTA SODAR NETWORK STUDY

ARB Sites were supported by the State of California Air Resources Board. NSF Sites were supported by the National Science Foundation, Research Applications Directorate.

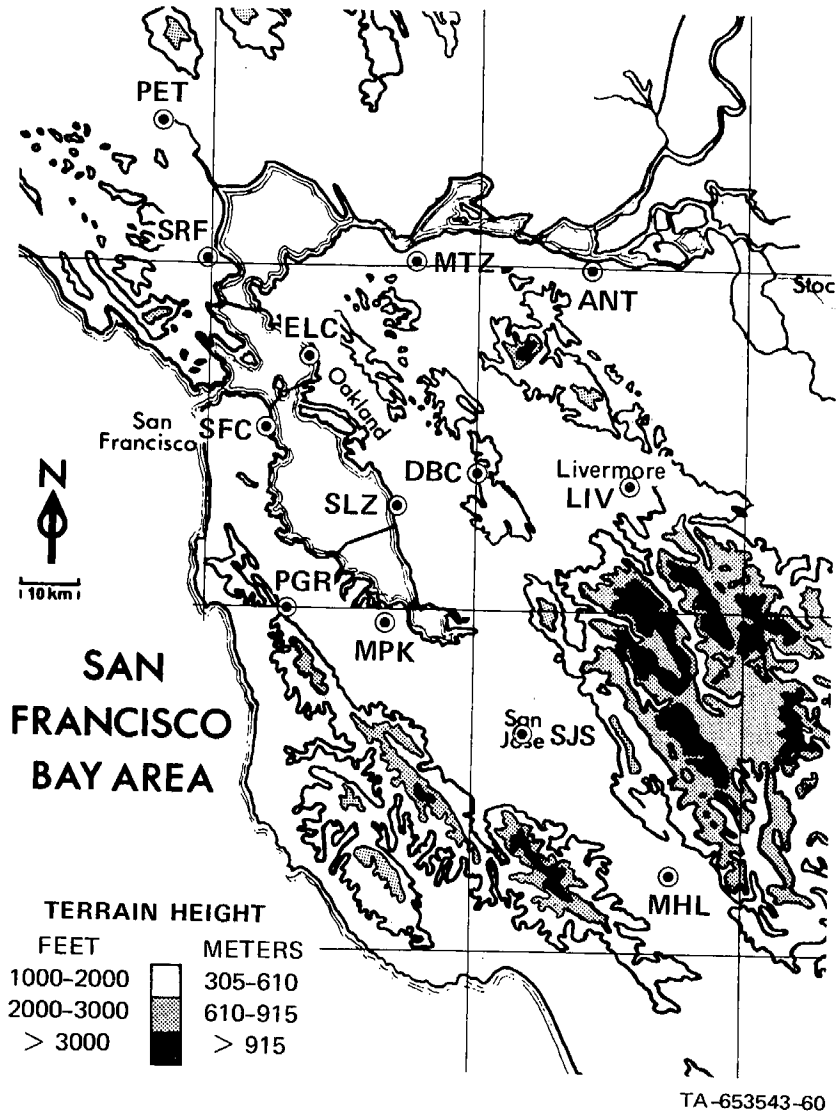
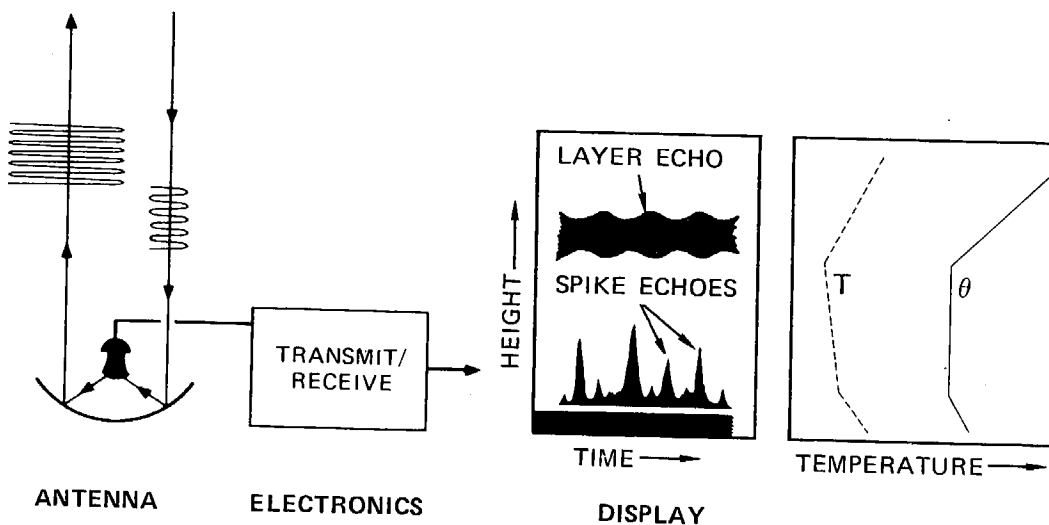


**FIGURE 2 TOPOGRAPHY OF SAN FRANCISCO BAY AREA**

Circled points mark location of sodars in 1976 network study.



TA-653522-115R

**FIGURE 3** SCHEMATIC REPRESENTATION OF THE MONOSTATIC SODAR METHOD, EQUIPMENT, AND ECHO TYPES  
 Profiles of temperature,  $T$ , and potential temperature,  $\theta$ , illustrate typical vertical gradients associated with each type of echo.

More detailed descriptions of these principles are given by Hall (1972), Tombach et al. (1973), Russell et al. (1974), and Parry et al. (1975), among others. For the purposes of the present study, the important point is that layer echoes mark regions of weak vertical mixing, while spike echoes mark regions of strong vertical mixing. On the other hand, the absence of acoustic echoes is ambiguous without further information, since this absence could result either from a near-adiabatic temperature profile (potentially strong mixing) or a complete absence of turbulence in a stable layer (extremely weak mixing).

### 3.3. The Bay Area Sodar Network Study and its Joint Sponsorship

The high incidence of strong, low, elevated inversions in the San Francisco Bay Area makes it an especially promising locale for sodar measurements. The strength and low altitude of these inversions not only make them easy to detect acoustically, but also increase their importance in determining pollutant concentrations. Moreover, the spatial and temporal variability of mixing depth, and the shortcomings of direct measurements cited in Section 3.1, enhance the desirability of continuous, remote measurements from a network of locations.

For these reasons SRI began in 1974 a three-year study of sodar applications to Bay Area air pollution problems. The first two years of the study were supported by the National Science Foundation (NSF Grant AEN73-02918-A01). Exploratory measurements were made with one sodar in 1974, and three sodars in 1975, together with supporting measurements by other sensors. The results of those early studies (Russell and Uthe, 1975, 1977a,b) guided the planning for a major field effort in 1976, which would employ about 12 sodars and aim to provide a representative data base on Bay Area mixing depth and stability, suitable for input to air quality simulation models.

Because of funding limitations, NSF was unable to provide sufficient funds to operate the complete 1976 network and reduce the data. Therefore, assistance was sought from the State of California Air Resources Board (ARB), as one of the potential users of the data base to be produced. Discussions and proposals between ARB and SRI in the spring of 1976 resulted in the present contract (A6-066-80), which provided partial support for 1976 sodar network operations and special data reduction tailored to the needs of ARB. Of the 13 sodars actually operated in the 1976 network, ARB funds supported operation of 5, stretching in an eastward arc from Petaluma on the north to Morgan Hill on the south (see Figure 1), while NSF funds supported 8 sodars clustered around San Francisco and San Pablo Bays.

### 3.4. Goals of this Project

The overall goal of this project was to produce a representative, smog-season data base on Bay Area mixing depth and near-surface stability, in a format suitable for automatic input to numerical air quality models. The subsidiary goals were:

- (1) To develop methods for acquiring and processing large volumes of sodar network data.
- (2) To evaluate the validity and usefulness of Bay Area sodar network data through comparisons with other measurements.
- (3) To use the resulting data set to develop new insights into the behavior of the mixing layer in the San Francisco Bay Area.

#### 4. PROCEDURE AND METHODOLOGY

##### 4.1. Site Selection, Sodar Tests, and Network Operation

A network of 13 sodars was established and operated from mid-August through the first few days of November 1976. The sites are shown in Figures 1 and 2 and listed in Table 1. With the exception of sites 8 and 12 (Pulgas Ridge and Dublin Canyon), each site was located on flat terrain, chosen to be representative of surrounding meteorological conditions. The Pulgas Ridge and Dublin Canyon sites were both located near the ridges of major hill ranges, in an effort to observe any influence of these hills and nearby gaps on inversion behavior.

Table 1  
1976 Sodar Network Sites

<u>No.</u>	<u>Code</u>	<u>Location</u>	<u>UTM Coordinates</u>		<u>Height ASL</u> (m)
			x(km)	y(km)	
1	PET	Petaluma	533	4232	3
2	MTZ	Martinez	579	4208	6
3	ANT	Antioch	608	4207	15
4	LIV	Livermore	616	4171	186
5	MHL	Morgan Hill	621	4104	98
6	SJS	San Jose	599	4132	68
7	MPK	Menlo Park	573	4145	18
8	PGR	Pulgas Ridge	559	4152	152
9	SFC	San Francisco	554	4182	8
10	SRF	San Rafael	542	4208	37
11	ELC	El Cerrito	560	4195	18
12	DBC	Dublin Canyon	591	4172	183
13	SLZ	San Lorenzo	595	4169	2

Before being deployed in the field, all 13 sodars were tested for several weeks at a single location and adjusted carefully to display the same acoustic echo structure when viewing the same atmosphere. Thereafter each sodar was installed in its acoustic enclosure in the field. At most sites homebuilt enclosures, using sand-filled plywood walls with foam lining, were used and found to be quite satisfactory. At other sites lead-lined enclosures, sold by the sodar manufacturer, were used. Each sodar was checked at approximately 2-day intervals

throughout the field program. These regular checks and the rapid performance of any necessary adjustments or repairs were crucial to the collection of a satisfactory data set. Details of enclosure construction, network setup, and maintenance are given by Russell (1976). Table 2 shows a log of successful data acquisition by time and site. Overall, a data capture rate of better than 95% was achieved.

#### 4.2. Ancillary Measurements

To test the validity of sodar-derived mixing parameters, ancillary measurements were made at each site on at least several days. The ancillary data included vertical temperature and humidity profiles measured by an SRI-instrumented aircraft, and haze and cloud vertical structure measured by mobile lidar. In addition wind speed and direction were measured at the Livermore site (No. 4) using a 10-m tower installed by SRI. Wind records for sites at or near Petaluma, Martinez, Antioch, and Morgan Hill (also on 10-m poles) were supplied by the California Department of Transportation (Caltrans). Table 2 shows a log of wind data that were successfully acquired and digitized. The ancillary measurements are described in more detail by Russell (1976b). The results are described in Section 6 and tabulated in Appendices B and C. In addition, a computer-card deck of the digital wind data has been delivered to ARB as specified by Contract A6-066-80.

#### 4.3. Sodar Data Processing

The very large volume (about 1000 site-days) of collected sodar data necessitated the development of special techniques to compress and store the data set, provide convenient access, convert it to the digital format required for model input, and summarize it in readily comprehensible form. A three-step process was implemented, as described below.

##### 4.3.1. Filming of Sodar Facsimile Records

Each 12-hour segment of facsimile record was photographed against a background that automatically included time and height scales and site and date identifiers. The entire data set was thus compressed to about three 3-inch rolls of 35-mm microfilm. Specific site-days could then be readily accessed using a microfilm reader. In fact, most significant features of acoustic echo structure could be viewed directly with the naked eye, thus permitting rapid scans of the data and comparisons of different sites and days.

A copy of this microfilm record has been delivered to ARB as specified by Contract A6-066-80.

Table 2  
1976 ACOUSTIC AND WIND NETWORK DATA LOG

SITE	AUGUST																																	
	1	2	3	4	5	6	7	8	9	10	11	12	13	14	15	16	17	18	19	20	21	22	23	24	25	26	27	28	29	30	31			
1. PETALUMA																																		
2. MARTINEZ																																		
3. ANTIOCH																																		
4. LIVERMORE																																		
5. MORGAN HILL																																		
6. SAN JOSE																																		
7. MENLO PARK																																		
8. PULGAS RIDGE																																		
9. SAN FRANCISCO																																		
10. SAN RAFAEL																																		
11. EL CERRITO																																		
12. DUBLIN CANYON																																		
13. SAN LORENZO																																		

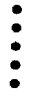
 Acoustic Data  
 Primary Wind Data  
 Secondary Wind Data (BAAPCD)  
 Secondary Wind Data (Calif. Div. of Forestry)

Table 2 (continued)  
 1976 ACOUSTIC AND WIND NETWORK DATA LOG

SITE	SEPTEMBER																														
	1	2	3	4	5	6	7	8	9	10	11	12	13	14	15	16	17	18	19	20	21	22	23	24	25	26	27	28	29	30	
1. PETALUMA	■																														
2. MARTINEZ	■	■	■	■	■	■	■	■	■	■	■	■	■	■	■	■	■	■	■	■	■	■	■	■	■	■	■	■	■	■	■
3. ANTIOCH	■	■	■	■	■	■	■	■	■	■	■	■	■	■	■	■	■	■	■	■	■	■	■	■	■	■	■	■	■	■	■
4. LIVERMORE	■	■	■	■	■	■	■	■	■	■	■	■	■	■	■	■	■	■	■	■	■	■	■	■	■	■	■	■	■	■	■
5. MORGAN HILL	■	■	■	■	■	■	■	■	■	■	■	■	■	■	■	■	■	■	■	■	■	■	■	■	■	■	■	■	■	■	■
6. SAN JOSE	■	■	■	■	■	■	■	■	■	■	■	■	■	■	■	■	■	■	■	■	■	■	■	■	■	■	■	■	■	■	■
7. MENLO PARK	■	■	■	■	■	■	■	■	■	■	■	■	■	■	■	■	■	■	■	■	■	■	■	■	■	■	■	■	■	■	■
8. PULGAS RIDGE	■	■	■	■	■	■	■	■	■	■	■	■	■	■	■	■	■	■	■	■	■	■	■	■	■	■	■	■	■	■	■
9. SAN FRANCISCO	■	■	■	■	■	■	■	■	■	■	■	■	■	■	■	■	■	■	■	■	■	■	■	■	■	■	■	■	■	■	■
10. SAN RAFAEL	■	■	■	■	■	■	■	■	■	■	■	■	■	■	■	■	■	■	■	■	■	■	■	■	■	■	■	■	■	■	■
11. EL CERRITO	■	■	■	■	■	■	■	■	■	■	■	■	■	■	■	■	■	■	■	■	■	■	■	■	■	■	■	■	■	■	■
12. DUBLIN CANYON	■	■	■	■	■	■	■	■	■	■	■	■	■	■	■	■	■	■	■	■	■	■	■	■	■	■	■	■	■	■	■
13. SAN LORENZO	■	■	■	■	■	■	■	■	■	■	■	■	■	■	■	■	■	■	■	■	■	■	■	■	■	■	■	■	■	■	■

 Acoustic Data  
 Primary Wind Data  
 Secondary Wind Data (BAAPCD)  
 Secondary Wind Data (Calif. Div. of Forestry)

Table 2 (continued)  
1976 ACOUSTIC AND WIND NETWORK DATA LOG

SITE	OCTOBER																															
	1	2	3	4	5	6	7	8	9	10	11	12	13	14	15	16	17	18	19	20	21	22	23	24	25	26	27	28	29	30	31	
1. PETALUMA																																
2. MARTINEZ																																
3. ANTIOCH																																
4. LIVERMORE																																
5. MORGAN HILL																																
6. SAN JOSE																																
7. MENLO PARK																																
8. PULGAS RIDGE																																
9. SAN FRANCISCO																																
10. SAN RAFAEL																																
11. EL CERRITO																																
12. DUBLIN CANYON																																
13. SAN LORENZO																																

 Acoustic Data  
 Primary Wind Data  
 Secondary Wind Data (BAAPCD)  
 Secondary Wind Data (Calif. Div. of Forestry)

Table 2 (concluded)  
 1976 ACOUSTIC AND WIND NETWORK DATA LOG

SITE	NOVEMBER											
	1	2	3	4	5	6	7	8	9	10	11	12
1. PETALUMA	■	■	■									
2. MARTINEZ	■	■	■									
3. ANTIOCH	■	■	■	■								
4. LIVERMORE	■	■	■	■	■	■	■	■	■	■	■	■
5. MORGAN HILL	■	■										
6. SAN JOSE	■	■										
7. MENLO PARK	■	■	■		■	■	■	■	■	■	■	■
8. PULGAS RIDGE	■	■			■	■	■	■	■	■	■	■
9. SAN FRANCISCO												
10. SAN RAFAEL	■	■	■									
11. EL CERRITO	■	■										
12. DUBLIN CANYON	■	■										
13. SAN LORENZO	■											

- Acoustic Data
- Primary Wind Data
- Secondary Wind Data (BAAPCD)
- Secondary Wind Data (Calif. Div. of Forestry)

#### 4.3.2. Digital Synopses of Sodar Records

A technique was developed for converting much of the sodar mixing depth and stability information to hourly digital parameters that can be easily input to a computer and comprehended by a human reader. As illustrated in Figure 4, three parameters are assigned to each one-hour period. The first parameter, set equal to the hourly-averaged height (in 10's of m above ground) of the lowest acoustic layer echo, provides a best-estimate of hourly-average mixing depth. (As explained below, the base height is read for elevated layers, and the top height for ground-based layers.) The second parameter, set equal to either "M" or "blank" indicates whether or not multiple layers are present. The third parameter, set equal to either "-", "1", or "blank", indicates whether a layer echo, spike echoes, or no echoes are present at the surface; it hence provides a coarse measure of the strength of vertical mixing near the surface. The complete code, including special parameter values for missing or ambiguous data is listed in Table 3.

Table 3

#### NUMBER AND SYMBOL CODE FOR DIGITAL SODAR DATA

(a) First Line or Card: Layer Heights and Multiple Layer Indicator

Entry	layer height indicator (first 2 columns of each hour)			multiple layer indicator (3rd column of each hour)	
	$1 \leq n \leq 98$	0	99	[blank]	M
Meaning	Height* of lowest layer echo in tens of meters	Questionable layer height† or missing data‡	No layer echo below 990 m	1 or fewer layer echoes present	2 or more layer echoes present

(b) Second Line or Card: Near-Surface Echo Type Indicator

Entry	-	[blank]	1	Q	X
Meaning	Layer echo	No echo	Spike echo	Questionable	Missing data

\* If layer is on ground (surface echo type indicator = -), "height" is height of layer top. If layer is aloft (surface echo type indicator = 1 or [blank]), "height" is height of layer top.

† If surface echo type indicator ≠ X

‡ If surface echo type indicator = X

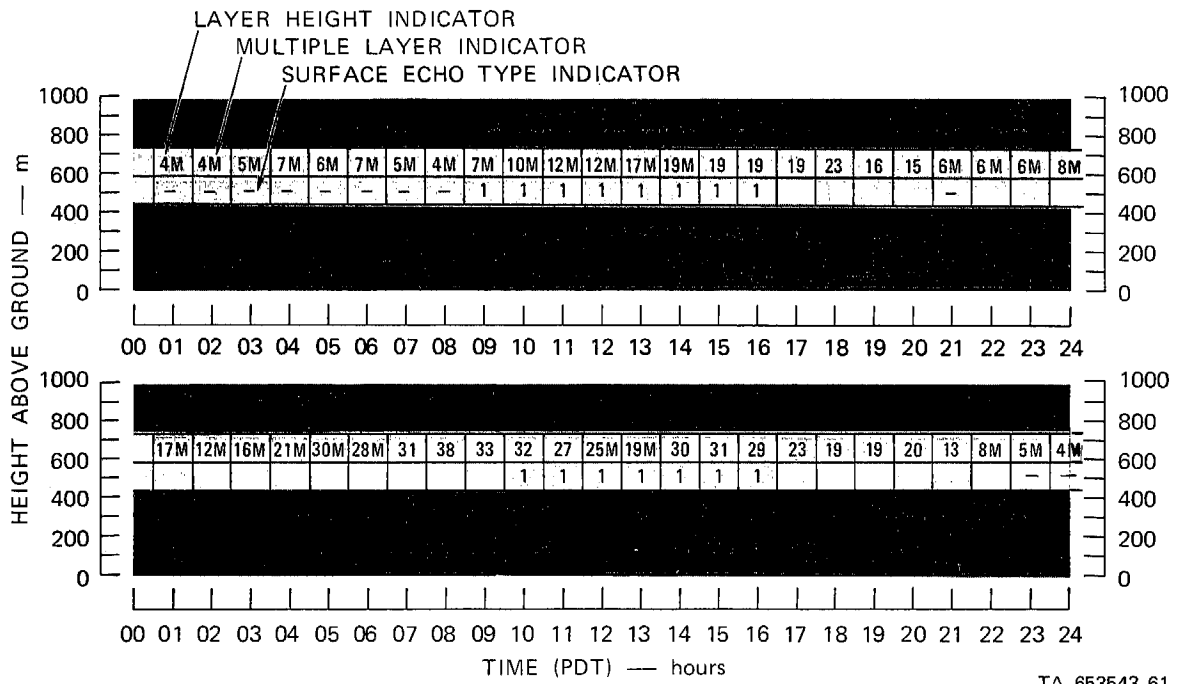


FIGURE 4 EXAMPLES OF SODAR FACSIMILE RECORDS, SHOWING THE METHOD USED TO MAKE HOURLY DIGITAL SYNOPSES OF ECHO HEIGHTS AND TYPES

The reason for using the base height of an elevated layer echo as the best estimate of mixing depth is that numerous measurements (see, e.g., Section 6.1) have shown that the layer echo base typically marks the base of an elevated layer of stable air (frequently an inversion; cf. Figure 3). Similarly, a ground-based layer echo indicates a ground-based stable layer. Many air quality models set mixing depth equal to zero when a ground-based stable layer is present, and this practice can be followed with the present data set simply by keying on the "-" surface echo type indicator. However, the occurrence of an acoustic echo does indicate that some turbulent mixing, albeit weak, is occurring up to the top height of the echo. Moreover, it is this turbulence (usually fed by wind shear) that mixes surface-cooled air upwards to deepen the ground-based stable layer. Surface-generated pollutants must be similarly mixed upwards by this turbulence. In fact, comparisons with lidar data have shown that, in the early morning, the top of the nocturnally-generated ground-based haze layer typically does coincide with the top of the acoustic layer echo, which is also the top of the ground-based stable layer (Russell et al., 1974). Hence, the top height of a ground-based layer echo does provide a measure of the upward limit of weak mixing in a stable layer, and is included in the data set for this reason.

The two lines of digital parameters shown in Figure 4 fit conveniently onto two 80-column computer cards. Thus, the entire data set of 1000 site-days can be compactly stored on about 2000 computer cards. Moreover, a site-month of data can be listed on a single page and stored in notebook form. We find that this permits quick scanning of large volumes of data to locate cases of interest. An example of one site-month of digital sodar data is shown in Table 4. A listing of all 1976 sodar data that were digitized is given in Appendix A. A computer-card deck of these data has been delivered to ARB, as specified in Contract A6-066-80.

#### 4.3.3. Maps of Sodar-Derived Mixing Depth

For any given time, the digital data described above can be written on a Bay Area map at appropriate locations, and contours drawn to show regional patterns of mixing depth or near-surface stability. These time-dependent maps aid comprehension of the large volume of numerical data and can reveal phenomena that might otherwise be missed. Examples are shown in Section 7.

Table 4

SAMPLE PRINTOUT OF DIGITAL SODAR DATA FOR ONE SITE-MONTH

SITE 4. LIVERMORE

UTMX=616, UTM Y=4171, SODAR HT=186 M ASL  
OCTOBER 1976

DAY	CLOCK HOUR (PACIFIC DAYLIGHT TIME)																										
	/	0	1	2	3	4	5	6	7	8	9	10	11	12	13	14	15	16	17	18	19	20	21	22	23	24	
1)	7M	8M	7M	8M	8M	7M	8M	9M	0	0	0	25M	27M	27M	32M	24M	99	99	30	14	0	16M	15M	26M	17M		
1)	-	-	-	-	-	-	-	Q	Q	Q	Q	1	1	1	1	1	1	1	1	1	1	1	1	1	1		
2)	17M	0	15M	23M	19M	10M	9M	10M	10	20	99	99	99	99	99	99	99	99	40	30	24M	14M	29M	29M	9M		
2)	-	Q	-	-	-	-	-	-	-	-	1	1	1	1	1	1	1	1	1	1	1	1	1	1	-		
3)	9M	5M	5M	11M	6M	5M	6M	4M	10M	27	50	55	57	67	99	99	99	99	99	99	8M	5M	5M	8M	7M	6M	
3)	-	-	-	-	-	-	-	-	-	-	1	1	1	1	1	1	1	1	1	1	1	1	1	1	-		
4)	6M	8M	6M	4M	4M	8M	5M	8M	5M	11M	12M	41	99	99	99	99	99	99	99	99	19	16M	5M	5M	5M	5M	
4)	-	-	-	-	-	-	-	-	-	-	1	1	1	1	1	1	1	1	1	1	1	1	1	1	-		
5)	5M	5M	6M	8M	4M	7M	5M	8M	9M	8M	9M	40	42	48	99	99	99	99	99	99	99	5	8	10	9M	5M	
5)	-	-	-	-	-	-	-	-	-	-	1	1	1	1	1	1	1	1	1	1	1	1	1	1	-		
6)	5M	7M	3M	3M	4M	12M	7M	6M	5M	8M	13M	20	38	25	40	41	42	42	44	6M	5M	5M	7M	6M	6M		
6)	-	-	-	-	-	-	-	-	-	-	1	1	1	1	1	1	1	1	1	1	1	1	1	1	-		
7)	6M	5M	5M	6M	8M	5M	6M	8M	8M	7M	10M	17M	44	51	47	99	99	99	99	15	7M	7M	7M	12M	9M	12M	
7)	-	-	-	-	-	-	-	-	-	-	1	1	1	1	1	1	1	1	1	1	1	1	1	1	-		
8)	12M	4M	9M	6M	9M	5M	6M	4M	6M	7M	11M	18M	23M	51	99	99	99	99	99	99	99	7M	5M	4M	11M	5M	
8)	-	-	-	-	-	-	-	-	-	-	1	1	1	1	1	1	1	1	1	1	1	1	1	1	-		
9)	5M	5M	6M	5M	6M	4M	4M	4M	5M	7M	11M	17M	41	44	43	99	99	99	99	99	7M	7M	6M	4M	4M	4M	
9)	-	-	-	-	-	-	-	-	-	-	1	1	1	1	1	1	1	1	1	1	1	1	1	1	-		
10)	4M	4M	3M	6M	7M	8M	19M	20M	21M	21M	27M	28M	28M	30M	39M	40M	40	41	11M	18M	8M	9M	13M	0	18M		
10)	-	-	-	-	-	-	-	-	-	-	1	1	1	1	1	1	1	1	1	1	1	1	1	1	Q		
11)	18M	10M	6M	5M	5M	5M	12M	12M	13M	10M	6M	59	55	68	99	99	99	99	99	12	7M	6M	5M	9M	7M	99	
11)	-	-	-	-	-	-	-	-	-	-	1	1	1	1	1	1	1	1	1	1	1	1	1	1	1		
12)	99	44M	32M	40M	49M	33M	40M	12M	32M	26M	40	34	32	99	99	99	99	99	99	99	99	5	5M	4M	5M	7M	
12)	1	1	1	1	1	1	1	1	1	1	1	1	1	1	1	1	1	1	1	1	1	1	1	1	-		
13)	7M	5M	4M	5M	4M	5M	5M	5M	4M	9M	10M	23	99	99	99	99	99	99	99	99	8	5M	4M	4M	4M	5M	
13)	-	-	-	-	-	-	-	-	-	-	1	1	1	1	1	1	1	1	1	1	1	1	1	1	-		
14)	5M	6M	5M	6M	6M	5M	5M	6M	10M	10M	8M	2133	99	99	99	99	99	99	99	20	9M	8M	10M	10M	8M	10M	
14)	-	-	-	-	-	-	-	-	-	-	1	1	1	1	1	1	1	1	1	1	1	1	1	1	-		
15)	10M	13M	7M	5M	5M	4M	5M	4M	4M	15M	13M	13M	18M	22	99	99	99	99	99	99	99	4M	6M	4M	5M	5M	
15)	-	-	-	-	-	-	-	-	-	-	1	1	1	1	1	1	1	1	1	1	1	1	1	1	-		
16)	5M	5M	8M	9M	10M	8M	7M	6M	9M	10M	10M	13M	24	99	99	99	99	99	99	99	8	7M	7M	8M	5M	6M	
16)	-	-	-	-	-	-	-	-	-	-	1	1	1	1	1	1	1	1	1	1	1	1	1	1	-		
17)	6M	6M	7M	7M	5M	7M	7M	5M	5M	6M	8M	8M	99	99	99	99	99	99	99	99	7M	5M	6M	6M	5M	5M	
17)	-	-	-	-	-	-	-	-	-	-	1	1	1	1	1	1	1	1	1	1	1	1	1	1	-		
18)	5M	5M	8M	6M	6M	6M	5M	6M	20M	23M	30M	29M	29M	37M	45	48	56	40	10M	10M	11M	9M	10M	9M	8M		
18)	-	-	-	-	-	-	-	-	-	-	1	1	1	1	1	1	1	1	1	1	1	1	1	1	-		
19)	8M	7M	7M	10M	30M	30M	31M	30M	27M	23M	20M	20M	20M	32	41	46	99	99	9	7M	6M	13M	19M	5M	5M		
19)	-	-	-	-	-	-	-	-	-	-	1	1	1	1	1	1	1	1	1	1	1	1	1	1	-		
20)	5M	7M	6M	9M	10M	5M	11M	9M	4M	8M	5M	99	99	99	99	99	99	99	99	99	0	0	10M	7M	9M	9M	
20)	-	-	-	-	-	-	-	-	-	-	1	1	1	1	1	1	1	1	1	1	1	1	1	1	-		
21)	9M	5M	5M	5M	5M	5M	5M	9M	0	0	0	0	0	0	0	0	0	0	99	7M	7M	5M	7M	6M	8M	10M	
21)	-	-	-	-	-	-	-	-	-	-	X	X	X	X	X	X	X	1	1	1	1	1	1	1	-		
22)	10M	10M	6M	6M	0M	0	43M	45M	45M	48M	51	49	50M	55M	51M	51M	55M	48M	10M	13M	13M	15M	0M	0M	0M	0M	
22)	-	-	-	-	Q	Q	-	-	-	-	1	1	1	1	1	1	1	1	1	1	1	1	1	1	1		
23)	0M	0M	0M	0M	0M	0M	0M	0M	0M	37M	37M	39M	42	53	52	68	45	30	8M	0M	0M	6M	0M	0M	30M		
23)	Q	Q	Q	Q	Q	Q	Q	Q	Q	1	1	1	1	1	1	1	1	1	1	1	1	1	1	1	-		
24)	30M	31M	41M	43M	43M	47M	48	48	51	51	50	49	50	54	43	99	99	99	99	0M	19M	34M	30M	63	22M	15M	
24)	-	-	-	-	-	-	-	-	-	-	1	1	1	1	1	1	1	1	1	1	1	1	1	1	-		
25)	15M	14M	10M	12M	9M	6M	63	53M	38M	25M	35M	62	85	70	99	99	99	99	99	99	10	5M	5M	7M	10M	0M	
25)	-	-	-	-	-	-	-	-	-	-	1	1	1	1	1	1	1	1	1	1	1	1	1	1	-		
26)	0M	0M	0M	0M	31	30	38	31	29	40	56	50	99	99	99	99	99	99	99	99	99	99	99	99	40	35	0M
26)	-	-	-	-	-	-	-	-	-	-	1	1	1	1	1	1	1	1	1	1	1	1	1	1	1	-	
27)	0M	5M	4M	5M	5M	6M	0M	6M	11M	21M	99	99	99	99	99	99	99	99	99	99	99	5M	5M	8M	5M	8M	5M
27)	-	-	-	-	-	-	-	-	-	-	1	1	1	1	1	1	1	1	1	1	1	1	1	1	1	-	
28)	5M	7M	7M	5M	4M	7M	7M	5M	6M	6M	11M	18M	27	99	99	99	99	99	99	99	8M	0M	4M	0M	0M	0M	10M
28)	-	-	-	-	-	-	-	-	-	-	1	1	1	1	1	1	1	1	1	1	1	1	1	1	1	-	
29)	10M	10M	5M	5M	5M	5M	5M	5M	6M	8M	11M	22M	28M	34	47	38	99	24	7M	5M	5M	0M	9M	6M	4M		
29)	-	-	-	-	-	-	-	-	-	-	1	1	1	1	1	1	1	1	1	1	1	1	1	1	1	-	
30)	4M	6M	6M	4M	4M	8M	10M	4M	6M	41M	30M	30M	35	99	99	99	99	99	99	99	8M	12M	11M	7M	6M	3M	8M
30)	-	-	-	-	-	-	-	-	-	-	1	1	1	1	1	1	1	1	1	1	1	1	1	1	1	-	
31)	8M	6M	0M	7M	0M	12M	8M	0M	8M	7M	13M	20	99	99	99	99	99	99	99	99	5M	7M	7M	8M	0M	0M	
31)	-	-	-	-	-	-	-	-	-	-	1	1	1	1	1	1	1	1	1	1	1	1	1	1	1	-	

## 5. DISTINCTION BETWEEN MARINE-CLASS AND LAND-CLASS DAILY SODAR RECORDS

In the 1974 and 1975 studies it became evident that the majority of Bay Area sodar records could be grouped into one of two major classes, and that this classification was very useful both for understanding boundary layer behavior and for roughly predicting pollution. The basis of this classification is described here, because it aids in understanding the 1976 data that follow.

The first class of daily sodar record, called land-class, is well exemplified by the record of 9 October 1976 at Morgan Hill (top row of Figure 4). This type of record is frequently observed at continental locations in the summer (e.g. Russell et al., 1974). It is characterized by a nocturnal ground-based layer echo which marks a stable layer formed by nocturnal radiative cooling of the ground. With morning solar heating of the ground, this stable layer is pushed aloft by convection, weakened, and sometimes destroyed. Accordingly, the morning acoustic record shows a rising and weakening layer echo above the spike echoes that mark convective cells rising from the surface.

The second class of sodar record, called marine-class, is well exemplified (up to 2000 PDT) by the Morgan Hill record of 10 October 1976 (bottom row of Figure 4). This type of record is typically observed in the Bay Area when the prevailing flow is from the ocean. Marine-class records are characterized by having a well-defined layer echo aloft for most of the record, and a near-absence of nocturnal ground-based layer echoes. The elevated layer echo marks the base of a subsidence inversion that caps a layer of inflowing marine air. Nocturnal stratus cloud decks frequently accompany this marine air (just below the inversion; see Section 6.2). Their reduction of nocturnal surface cooling, together with the influx of cool air below the clouds, probably explains the lack of formation of surface-based stable layers. In fact, at some Bay Area locations, marine-class sodar records frequently show nocturnal spike echoes, suggesting nighttime convective activity. (For examples see Russell and Uthe, 1977b.)

As a rule, Bay Area days with land-class sodar records at most sites tend to be more polluted than days with marine-class sodar records at most sites. This result, which evidently applies to both primary and secondary pollutants, can appear to contradict the fact that midday mixing depths on land-class days frequently exceed those on marine-class days. (This occurs because the marine-class subsidence inversion typically descends to its daily minimum altitude shortly after noon, whereas the land-class rising inversion attains its maximum height or is eroded completely away at this time.) The explanation for the smaller pollution concentrations on marine-class days evidently lies in the greater depth and intensity of mixing in the night and early morning hours, together with the influx of cleaner marine air. (For further discussion see Section 7 and Russell and Uthe, 1977a,b.)

## 6. VALIDITY OF SODAR-INFERRED MIXING DEPTHS

### 6.1. Relation to Temperature and Humidity Profiles

Numerous comparisons were made between mixing depths inferred from the sodar records (as shown in Section 4.3.2) and from simultaneously measured temperature and humidity profiles. The 1976 temperature and humidity profiles were measured by a light airplane, specially instrumented by SRI and flown in spirals over each sodar site. (The airplane data are plotted in Appendix C; airplane routes are given by Russell, 1976b.) Mixing depths were evaluated from the airplane and sodar data by different people, working at different times, to eliminate bias toward agreement of the two types of measurements. In addition, for half of the data set, each airplane mixing depth was evaluated by three different people (two meteorologists and a physicist), also working independently, to provide a measure of the uncertainty in mixing depths inferred from temperature and humidity profiles.

As will be seen, this uncertainty can be quite large for late afternoon, evening, or nighttime temperature profiles, because at these times several weak inversions or isothermal layers can often appear at different heights in a single profile. We have found that, in such cases, different meteorologists often pick different features as mixing depth indicators. In some cases, each meteorologist is also quite uncertain, giving "best-guess," "upper-bound", and "lower-bound" mixing depths that differ by as much as several hundred meters or more. Figure 5 shows six examples of this type, along with the inferred mixing depths. (The rule for inferring mixing depth when a ground-based stable layer is present is as explained in Section 4.3.2. That is, the height to which turbulence has mixed surface-cooled air aloft is taken as the mixing depth.)

Another point illustrated by Figure 5 is that, in the late afternoon and evening, relative humidity or water vapor mixing ratio profiles may not give a valid indication of instantaneous mixing depth. (Note, for example, the lack of features at the mixing depth in the first and last humidity profiles of the second row. Mixing ratio profiles were very similar to the humidity profiles--see Appendix C.) This lack of features occurs because late afternoon and evening humidity profiles are frequently the result of mixing processes that occurred earlier in the day, when mixing was much stronger and deeper. This same fact applies to late afternoon and evening haze profiles--as noted by Russell et al. (1974) and also in Section 5.2.

The results of the 1976 sodar-vs-airplane mixing depth comparisons are summarized as a scatter diagram in Figure 6. (The "airplane" coordinate of each data point is the mean of the best-guess mixing depths picked by different evaluators.) As can be seen, the overall agreement between the airplane and sodar data is reasonably good, and little or no systematic difference is evident. However, there is appreciable scatter in the data set, caused by notable disagreements in certain individual cases. It is important to emphasize that much of this scatter is caused

by uncertainty in airplane-inferred mixing depths, as illustrated in Figure 5. The horizontal error bars in Figure 6 indicate this uncertainty by spanning the range between best-guess mixing depths inferred from the same temperature profile by different evaluators, or the range between upper and lower bounds picked by a single evaluator. The cases shown in Figure 5 are examples that yielded some of the largest error bars in Figure 6.

It should be noted that the 1976 sodar-airplane comparisons can be expected to yield larger differences in inferred mixing depth than would result from comparisons equally distributed throughout a 24-hour diurnal

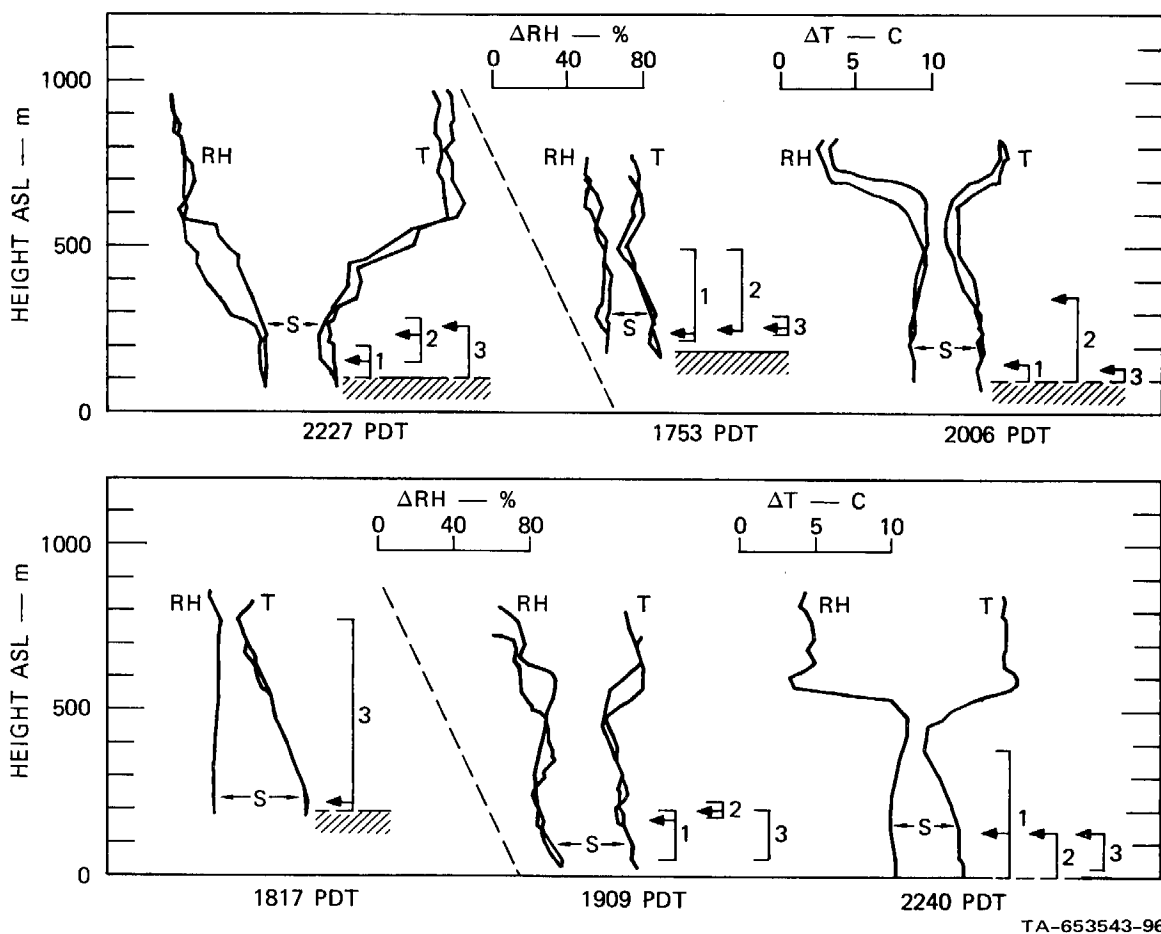
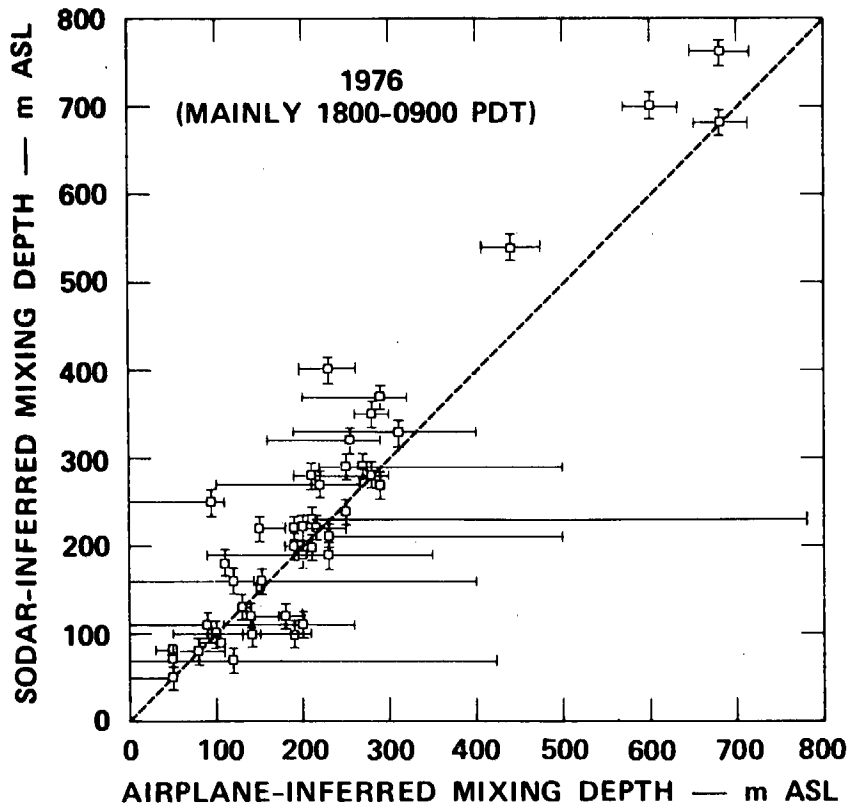


FIGURE 5 EXAMPLES OF TEMPERATURE AND HUMIDITY PROFILES AND INFERRED MIXING DEPTHS

Brackets with arrows indicate upper-bound, lower-bound, and best-guess mixing depths inferred from T and RH profiles independently by three different evaluators. "S" indicates sodar-inferred mixing depth. Double profiles are from airplane ascent and descent. Dashed lines are dry adiabats.

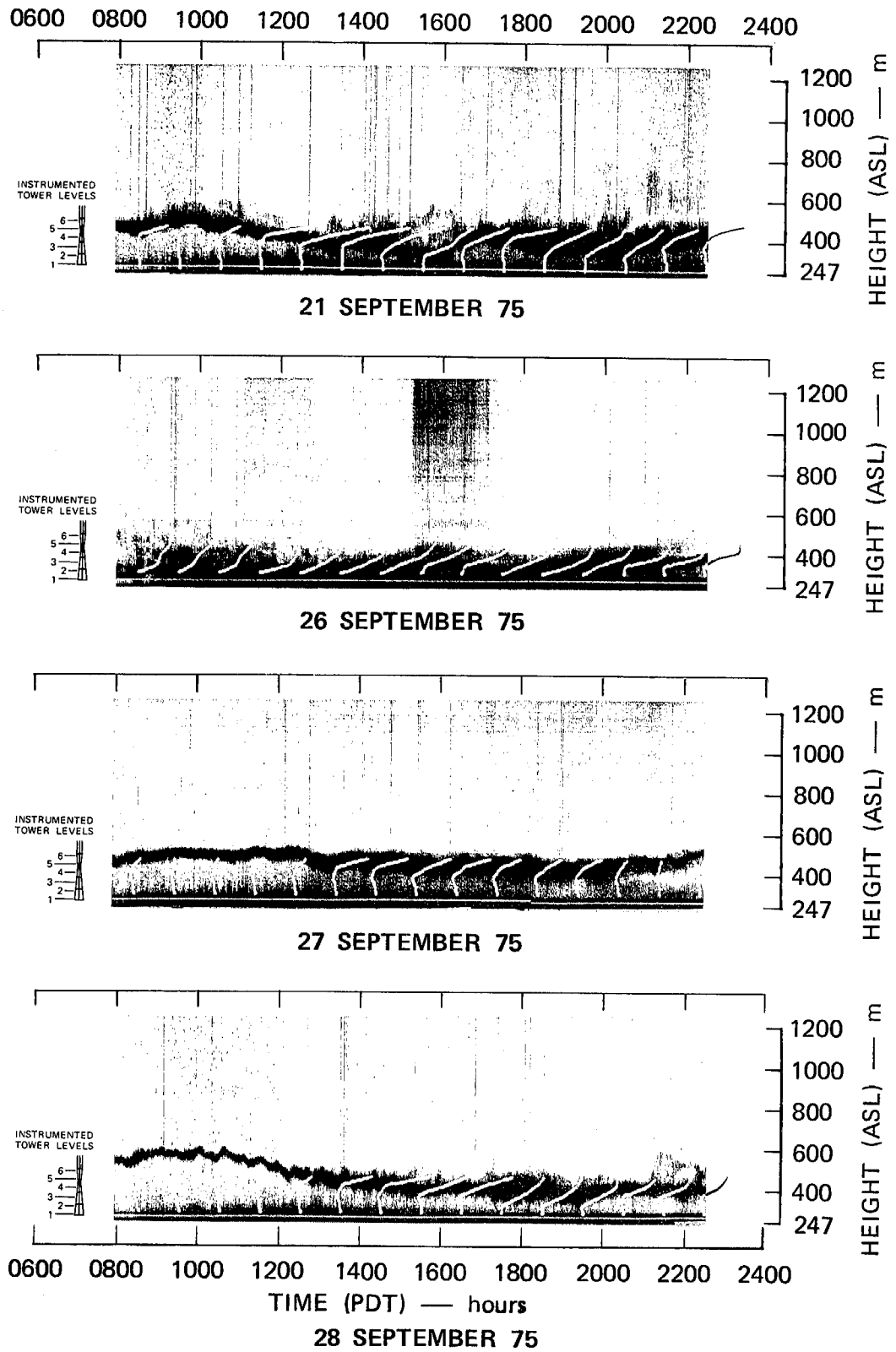
cycle. The 1976 airplane flights were scheduled predominantly in the late afternoon, evening, and nighttime hours, in order to focus on a time when weak or multiple echo layers contribute ambiguity to sodar-inferred mixing depths. One result of our 1976 comparisons is to point out that temperature and humidity profiles (especially those measured in late afternoon, evening, and nighttime) can also be quite ambiguous to interpret in terms of mixing depth.

During daytime in the Bay Area, both sodar records and temperature profiles are usually easier to interpret in terms of mixing depth, because there is usually a single (often strong) inversion aloft, giving rise to a single (often strong) acoustic layer echo. Our 1975, predominantly daytime comparisons (using tower, airplane, and balloon data) demonstrated this lack of ambiguity, as well as quite good agreement between sodar- and temperature-inferred mixing depths. Examples of these 1975 comparisons are shown in Figures 7 and 8. The complete 1975



TA-653543-59R1

FIGURE 6 COMPARISON OF MIXING DEPTHS INFERRED FROM 1976 SODAR AND AIRPLANE MEASUREMENTS



TA-653543-49

FIGURE 7 COMPARISON BETWEEN ACOUSTIC ECHO STRUCTURE AND TOWER-MEASURED TEMPERATURE PROFILES

Profiles are hourly averages centered at time below profile base.

# STANFORD

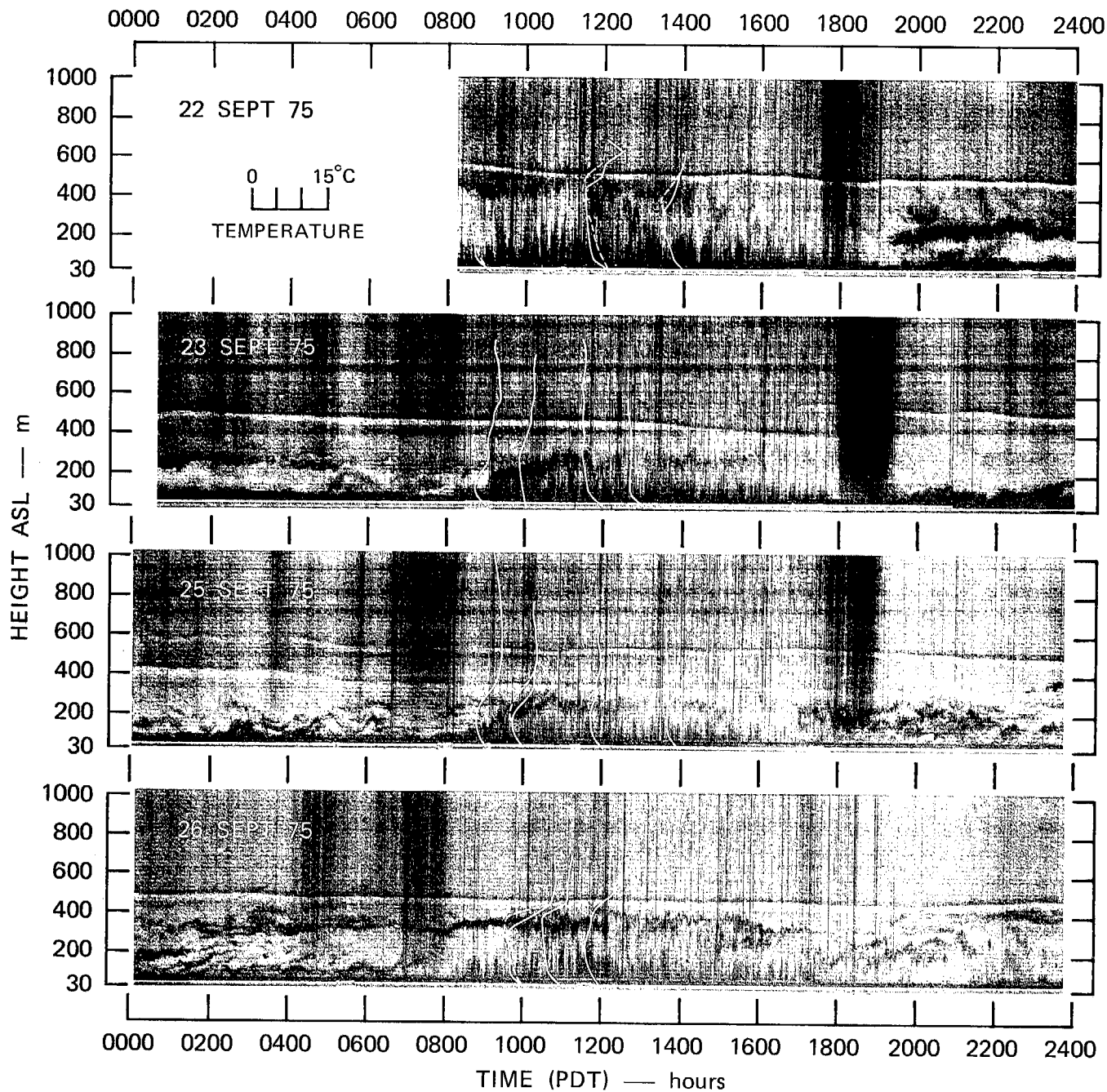
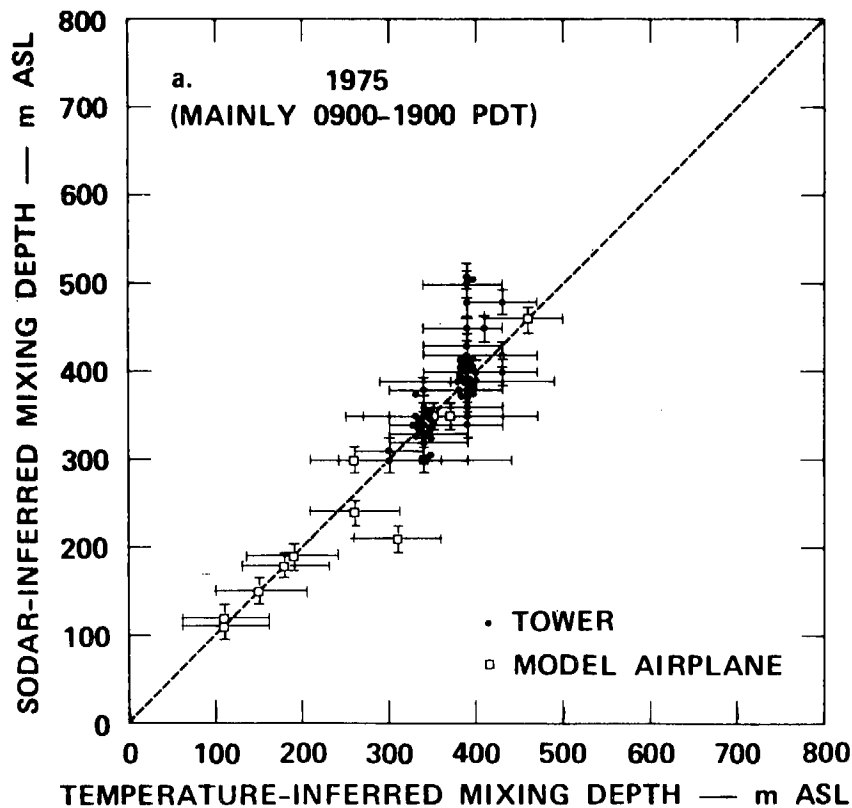


FIGURE 8 COMPARISON BETWEEN ACOUSTIC ECHO STRUCTURE AND MODEL-AIRPLANE-MEASURED TEMPERATURE PROFILES

Profiles were measured at time shown below profile base. Ignore the dark-above-light lines marked "paper bulge effect". These lines were caused by a bulge in the chart paper and do not indicate atmospheric echoes.

comparisons are also summarized as a scatter diagram in Figure 9. As expected, the scatter of data points is appreciably less for the 1975, predominantly daytime, data set, than for the 1976, predominantly nocturnal one.

Taken together, the data of Figures 5-9 provide rather strong support for the overall validity of mixing depths inferred from Bay Area sodar data, and for their use in air quality prediction schemes. This is especially so when one considers the possible shortcomings of alternate techniques (for example, the ambiguities of temperature and humidity profiles illustrated in Figure 5).



TA-653543-59R2

FIGURE 9 COMPARISON OF MIXING DEPTHS INFERRED FROM 1975 SODAR AND TEMPERATURE-PROFILE MEASUREMENTS

## 6.2. Relation to Haze and Cloud Structure

Numerous comparisons were also made between the sodar records and the haze and cloud structure revealed by lidar measurements. Figure 10 shows an example of one such comparison, made on a marine-class day by using a special system (Uthe and Allen, 1975) that simultaneously displays the lidar and sodar data on a television screen. (Hence, for this example alone, increasing brightness--not darkness--indicates increasing signal strength.) The dark outlines in the lidar data below 300 m and between 0800 and 1000 PDT mark the edges of a stratus cloud deck. They are caused by the strong signals from the cloud edges overflowing the brightest gray-step of the display and being reset to the darkest gray-step (black). The even stronger signals from the core of the cloud, even after being reset to compensate for overflow, produce a bright display, yielding the white core shown. All other lidar signals shown result from haze and smog.

Figure 10 is a fairly typical example of lidar and sodar data for a marine-class day. There is good agreement between the top height of the morning stratus cloud deck and the base height of the elevated acoustic layer echo. Similarly, just after the cloud dissipates, there is good agreement between the haze top height and the base of the layer echo. In the example shown, this agreement continues even when the sodar layer echo descends, between 1100 and 1430 PDT. However, this last result is not general, and in some marine-class cases the afternoon haze top does remain near the level established in the morning while the sodar layer echo (subsidence inversion base) descends to a lower height. In such a case the lidar-depicted afternoon haze top is primarily a measure of previous mixing history, rather than the instantaneous limit to vertical mixing that is revealed by the sodar data. (Recall the similar case with afternoon and evening humidity profiles, discussed in Section 6.1.)

Numerous comparisons such as that shown in Figure 10 strongly support the idea that, on marine-class days, the base of the daytime acoustic layer echo does indeed represent the instantaneous limit to vertical mixing (or, more properly, the height at which vertical mixing suddenly becomes much weaker--Goodman and Miller, 1977). Other comparisons on land-class days also support the mixing inferences embodied in the digitization scheme of Figure 4. However, they also indicate that, when the mixing top is weakened by convection and pushed to more than about 600 m above ground, the moderately-powered sodars used in this study may be unable to detect this weak top. This is a case in which the lidar is the superior detector of instantaneous mixing depth, since the rising haze top (easily detected by the lidar) is, in such a case, a good measure of the instantaneous mixing limit. For examples and further discussion, see Russell et al. (1974) and Russell and Uthe (1975).

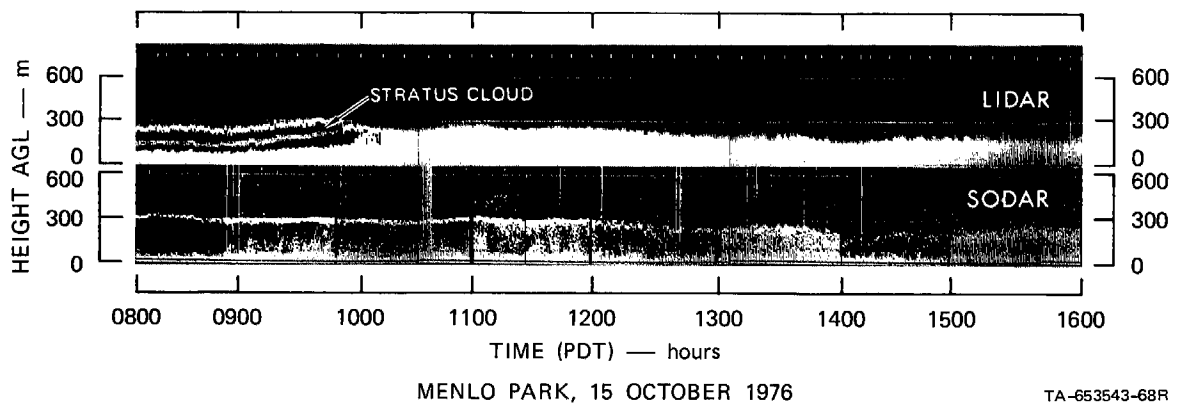


FIGURE 10 TELEVISION DISPLAY OF SIMULTANEOUSLY MEASURED LIDAR AND SODAR DATA

## 7. SODAR-DERIVED MIXING DEPTH MAPS FOR CONSECUTIVE HIGH- AND LOW-OXIDANT DAYS

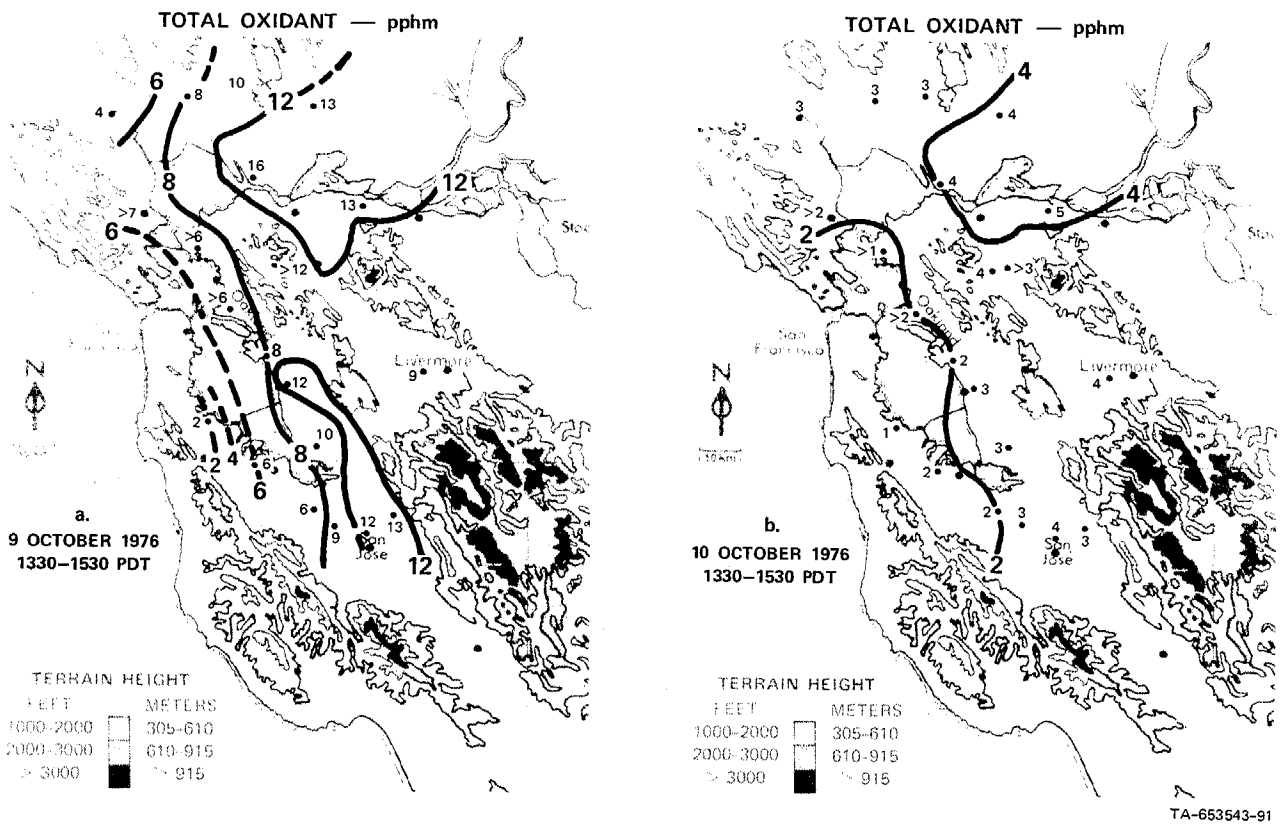
To illustrate the type of information contained in the digitized sodar network data, we show an example of time-dependent contour maps of mixing depth derived therefrom. All maps shown are for selected times on 9 and 10 October, 1976, a Saturday and Sunday for which sodar records at a single site have already been shown in Figure 4. For reference, Figure 11 shows contours of afternoon total oxidant concentration, derived from Bay Area Air Pollution Control District network measurements. As can be seen, the federal hourly-average oxidant standard of 8 pphm was exceeded at many locations on 9 October, but concentrations were much less on 10 October. During the preceding week (5-8 October) conditions were similar to 9 October, and the federal oxidant standard was exceeded many times at many Bay Area monitoring stations.

Figure 12a shows contours of mixing depth measured between 0730 and 0930 PDT on 9 October. These early morning contours of mixing depth follow the contours of Bay Area topography quite closely, with a low over the bays. Throughout the predawn hours of 8 October and the night of 8-9 October (not shown) a very similar pattern, with slightly smaller mixing depths, was observed. Nearly all of the sodars showed ground-based stable layers nearly all of the time in this period (as in the top row of Figure 4). Note that the contour heights are in meters above sea level (ASL)/1/. The greater mixing heights in the Livermore Valley are caused by the higher ground level (150-190 m ASL) there. At all sites the thickness of the mixing layer above ground was less than 100 m throughout most nighttime hours prior to 0730 PDT on 9 October. When compared to the nighttime values, the contours of Figure 12a show a slight rise at nearly all stations, caused by the morning start of solar surface heating. Nevertheless, during this period when many primary pollutants are emitted near ground level, mixing depths were restricted to less than 150 m above ground at nearly all sites.

Figure 12b shows a continuing increase in mixing depth at all sites through 1130 PDT. It appears that the region of rise includes the bays, and the <100-m low that had been there evidently disappears during this period. (This is admittedly an extrapolation, based on measurements at the five sites--ELC, SLZ, MPK, SFC, and SRF--near the bay shores.)

Between 1130 and 1330 PDT (not shown) the increase in mixing depth at all heated land areas continued. However, it is interesting to note that a lowering occurred over the bays and their shores, evidently in compensation for the rising air over heated land areas. This situation continued through 1530 PDT, as shown in Figure 12c. (Note the return of the 100-m contour along the bay shores.) We note also that the shapes

/1/ Small numbers by individual sites show mixing depths (ASL) at those sites. An accompanying arrow or bar indicates spike echoes or a ground-based layer echo, respectively. In some cases two small numbers are written beside a site. This indicates a transition that occurred during the two-hour period of the map.



**FIGURE 11** CONTOUR MAPS OF TOTAL OXIDANT MEASURED AT BAAPCD MONITORING STATIONS, 1330-1530 PDT, 9 AND 10 OCTOBER 1976

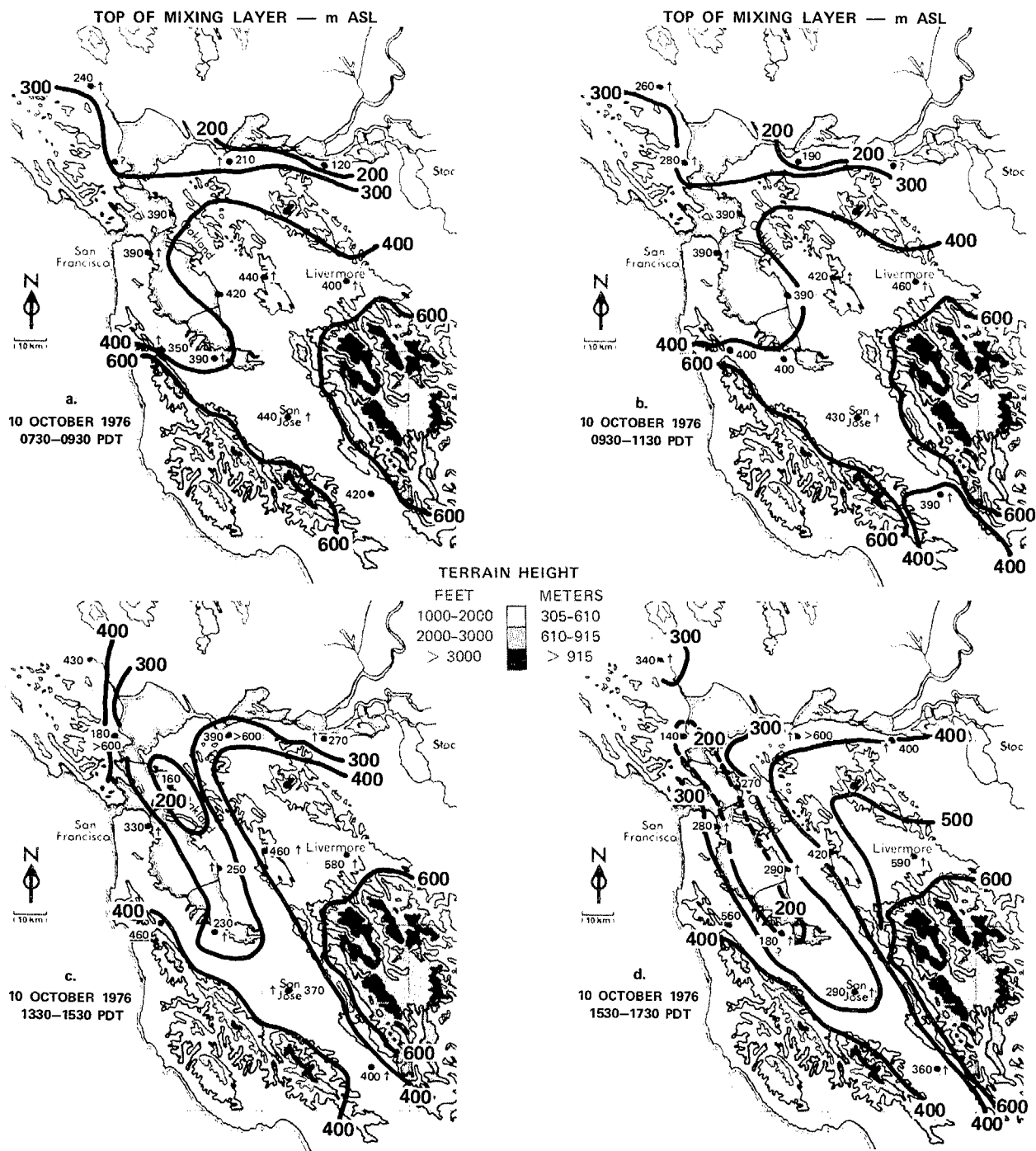


and heights of the contours shown in Figure 9c are quite similar to those derived from airplane data by Ahrens and Miller (1969) in a previous study.

By the 1530-1730 PDT period (Figure 12d) a decrease in mixing depth had begun throughout the major valley stretching from Petaluma (PET; Figure 2), down the bays, and to Morgan Hill (MHL). Meanwhile, however, the mixing top height continued to exceed 600 m ASL in the more inland Livermore Valley, and no lowering was evident. Within the next two hours (1730-1930 PDT; not shown), ground-based stable layers had formed at most sites, and the mixing depth contour maps until 2330 PDT were all similar to that shown for 0730-0930 PDT (Figure 12a), with slightly smaller depths and a larger <100-m area over the bays.

Between 2330 PDT on 9 October and 0130 PDT on 10 October (not shown) a sudden lifting of the top of the mixing layer occurred at San Francisco, Petaluma, and Morgan Hill (see Figure 4, bottom row). This lifting continued to penetrate inland throughout the predawn hours, and by 0730-0930 PDT (Figure 13a) mixing depths at all sites but Antioch exceeded by 90 to 310 m their values during the same period on 9 October (Figure 12a). Similar large mixing depths persisted through 1130 PDT (Figure 13b). It is interesting to note that during this time the mixing depth contours do not follow the contours of Bay Area topography to the extent that they did on 9 October. This suggests that boundary-layer depth early on 10 October (a marine-class day) was determined by a large-scale forcing that did not originate within the Bay Area (unlike the local solar heating that controlled boundary layer growth on 9 October, a land-class day).

Between 1130 and 1330 PDT on 10 October (not shown) mixing depths began to decrease in a trough over and just east of the bays. This trough spread to many surrounding sites between 1330 and 1730 PDT, as shown in Figures 13c and 13d. As discussed in Section 5 (see especially Figures 4, 7, and 10), this late-morning and early-afternoon decrease of mixing depth is typical of marine-class days. Because of the decrease, afternoon mixing depths at some sites were actually less on 10 October than they were at the same time on the much more polluted 9 October. (Compare Figures 13c,d with Figures 12c,d.) As discussed in Section 5, evidently the mixing conditions during the morning hours of 9 and 10 October had a strong influence on the oxidant concentrations that developed in the afternoons of those days. Of course, the influx of marine air that doubtless accompanied the lifting during the night of 9-10 October probably also played a major role.



TA-653543-93

FIGURE 13 CONTOURS OF MIXING DEPTH DERIVED FROM SODAR NETWORK, 10 OCTOBER 1976

## REFERENCES

- Ahrens, D., and A. Miller, 1969: Variations of the temperature inversion over the San Francisco Bay Area. San Jose State College Department of Meteorology, San Jose, California.
- Goodman, J.K., and A. Miller, 1977: Mass transport across a temperature inversion. J. Geophys. Res., 82, 3463-3471.
- Hall, F.F. Jr., 1972: Temperature and wind structure studies by acoustic echo-sounding. Chapter 18 of Remote Sensing of the Troposphere, V.E. Derr, ed., U.S. Department of Commerce. For sale by Superintendent of Documents, U.S. Government Printing Office, Washington, D.C. 20402.
- MacCracken, M.C. and G. D. Sauter, 1975: Development of an air pollution model for the San Francisco Bay Area. Lawrence Livermore Laboratory, Report UCRL-51920. Available from National Technical Information Service, Springfield, VA., 22151.
- Parry, H.D., M. J. Sanders, and H.D. Jensen, 1975: Operational applications of a pure acoustic sounding system. J. Appl. Meteor., 14, 67-77.
- Russell, P.B., 1976a: Marine boundary layer behavior measured by a network of sodars (acoustic radars) in the San Francisco Bay Area. Proceedings, Navy Workshop on Remote Sensing of the Marine Boundary Layer, Vail, Colorado, 9-11 August 1976. Published by Naval Research Laboratory, Arlington, Va.
- Russell, P. B., 1976b, 1977: Development of a vertical mixing data base in the San Francisco Bay and Delta Region. First and Second Quarterly Reports, to State of California Air Resources Board, Project 5721, SRI International, Menlo Park, California 94025.
- Russell, P. B., and E. E. Uthe, 1975: Development of an acoustic sounder network for air pollution and land use applications, Post-workshop mini-paper volume, Third Workshop in Atmospheric Acoustics, June 1975, Toronto, Canada. Available from the authors as Progress Report II, Project 3442. SRI International, Menlo Park, California 94025.
- Russell, P.B., and E.E. Uthe, 1977a: Sodar network measurements of regional mixing depth and stability patterns for an air quality model. Preprint Volume, AMS/APCA Conf. Appl. Air Poll. Meteor., pp. 72-79, Published by Amer. Meteor. Soc., Boston, MA, 02108, and available from the authors, SRI International, Menlo Park, CA, 94025.
- Russell, P. B., and E. E. Uthe, 1977b: Acoustic and direct measurements of atmospheric mixing at three sites during an air pollution incident. Atmos. Environ., in press.

- Russell, P. B., E. E. Uthe, F. L. Ludwig, and N. A. Shaw, 1974: A comparison of atmospheric structure as observed with monostatic acoustic sounder and lidar techniques. J. Geophys. Res., 79, 5555-5556.
- Tombach, I., P. B. MacCready, and L. Baboolal, 1973: Use of a monostatic acoustic sounder in air pollution diffusion estimates. Second Joint Conference on Sensing of Environmental Pollutants, Washington, D.C., 10-12 December 1973. Reprints available from Instrument Society of America, 400 Stanwix St., Pittsburgh, PA 15222.
- Uthe, E.E., 1976: The SRI Mark IX Mobile Lidar System and its applications. Navy Workshop on Remote Sensing of the Marine Boundary Layer, Vail, Colorado, 9-11 August 1976.
- Uthe, E.E., and R.J. Allen, 1975: A digital real-time lidar data recording, processing and display system. Opt. Quantum Electron., 7, 121-129.
- Wesley, M.L., 1976: The combined effect of temperature and humidity fluctuations on refractive index. J. Appl. Meteor., 12, 1192, 1204.

PUBLICATION RESULTING FROM THIS PROJECT

Russell, P.B., and E.E. Uthe, 1977: Sodar network measurements of regional mixing depth and stability patterns for an air quality model. Preprint Volume, AMS/APCA Conf. Appl. Air Poll. Meteor., pp. 72-79. Published by Amer. Meteor. Soc., Boston, MA, 02108, and available from the authors, SRI International, Menlo Park, CA, 94015.